



The long intergenic noncoding RNA ARES modulates root architecture in Arabidopsis

Thomas Roulé, María Florencia Legascue, Andana Barrios, Nicolás Gaggion, Martin Crespi, Federico Ariel, Thomas Blein

► To cite this version:

Thomas Roulé, María Florencia Legascue, Andana Barrios, Nicolás Gaggion, Martin Crespi, et al.. The long intergenic noncoding RNA ARES modulates root architecture in Arabidopsis. IUBMB Life, 2023, 75 (10), pp.880-892. 10.1002/iub.2761 . hal-04299803

HAL Id: hal-04299803

<https://hal.science/hal-04299803>

Submitted on 22 Nov 2023

HAL is a multi-disciplinary open access archive for the deposit and dissemination of scientific research documents, whether they are published or not. The documents may come from teaching and research institutions in France or abroad, or from public or private research centers.

L'archive ouverte pluridisciplinaire **HAL**, est destinée au dépôt et à la diffusion de documents scientifiques de niveau recherche, publiés ou non, émanant des établissements d'enseignement et de recherche français ou étrangers, des laboratoires publics ou privés.

The long intergenic noncoding RNA *ARES* modulates root architecture in Arabidopsis

Thomas Roulé^{1,2}  | María Florencia Legascue³ | Andana Barrios^{1,2,3} |
Nicolás Gaggion⁴  | Martin Crespi^{1,2}  | Federico Ariel³  | Thomas Blein^{1,2} 

¹Institute of Plant Sciences Paris Saclay IPS2, CNRS, INRA, Université Evry, Université Paris-Saclay, Gif-sur-Yvette, France

²Institute of Plant Sciences Paris-Saclay IPS2, Université de Paris, Gif-sur-Yvette, France

³Instituto de Agrobiotecnología del Litoral, CONICET, Universidad Nacional del Litoral, Santa Fe, Argentina

⁴Institute for Signals, Systems and Computational Intelligence, sinc(i) CONICET-Universidad Nacional del Litoral, Santa Fe, Argentina

Correspondence

Federico Ariel, Instituto de Agrobiotecnología del Litoral, CONICET, Universidad Nacional del Litoral, Colectora Ruta Nacional 168 km 0, 3000 Santa Fe, Argentina.
Email: farriel@santafe-conicet.gov.ar

Thomas Blein, Institute of Plant Sciences Paris Saclay IPS2, CNRS, INRA, Université Evry, Université Paris-Saclay, Bâtiment 630, 91190 Gif-sur-Yvette, France.
Email: thomas.blein@cnrs.fr

Funding information

Agence Nationale de la Recherche, Grant/Award Number: ANR-17-EUR-0007; ECOS-SUD, Grant/Award Number: A20N05; International Centre for Genetic Engineering and Biotechnology, Grant/Award Number: ICGEB CRP-ARG01; Ministère de l'Enseignement supérieur, de la Recherche et de l'Innovation; Proyecto de Investigación Científica y Tecnológica, Grant/Award Number: PICT2019-4137

Abstract

Long noncoding RNAs (lncRNAs) have emerged as important regulators of gene expression in plants. They have been linked to a wide range of molecular mechanisms, including epigenetics, miRNA activity, RNA processing and translation, and protein localization or stability. In Arabidopsis, characterized lncRNAs have been implicated in several physiological contexts, including plant development and the response to the environment. Here we searched for lncRNA loci located nearby key genes involved in root development and identified the lncRNA *ARES* (*AUXIN REGULATOR ELEMENT DOWNSTREAM SOLITARYROOT*) downstream of the lateral root master gene *IAA14/SOLITARYROOT* (*SLR*). Although *ARES* and *IAA14* are co-regulated during development, the knockdown and knockout of *ARES* did not affect *IAA14* expression. However, in response to exogenous auxin, *ARES* knockdown impairs the induction of its other neighboring gene encoding the transcription factor NF-YB3. Furthermore, knockdown/out of *ARES* results in a root developmental phenotype in control conditions. Accordingly, a transcriptomic analysis revealed that a subset of *ARF7*-dependent genes is deregulated. Altogether, our results hint at the lncRNA *ARES* as a novel regulator of the auxin response governing lateral root development, likely by modulating gene expression in *trans*.

Abbreviations: *ARES*, Auxin regulator element downstream solitaryroot; *ARF*, Auxin Response Factor; Aux/IAA, Auxin/Indole-3-Acetic Acid; DCL3, Dicer-like 3; DEG, differentially expressed genes; GO, Gene Ontology; HPA1, Histidinol phosphate aminotransferase 1; HSP20-like, Heat shock protein 20-like; IAA1, Indole-3-acetic acid inducible 1; IAA3, Indole-3-acetic acid inducible 3; IAA14, Indole-3-acetic acid inducible 14; IAA19, Indole-3-acetic acid inducible 19; lincRNA, long intergenic noncoding RNA; lncRNA, long noncoding RNA; NF-YB3, Nuclear factor Y, Subunit B3; NAA, 1-Naphthaleneacetic acid; NAT, natural antisense transcript; NPA, Naphthylphthalamic acid; NRPD2A, Nuclear RNA polymerase D2A; NRPD1A, Nuclear RNA polymerase D1A; PIP5K, Phosphatidylinositol 4-phosphate 5-kinase; RNAi, RNA interference; RdDM, RNA-directed DNA methylation; SHY2, Short hypocotyl 2; SLR, Solitaryroot; TSS, Transcription Start Site.

This is an open access article under the terms of the [Creative Commons Attribution-NonCommercial](https://creativecommons.org/licenses/by-nc/4.0/) License, which permits use, distribution and reproduction in any medium, provided the original work is properly cited and is not used for commercial purposes.

© 2023 The Authors. *IUBMB Life* published by Wiley Periodicals LLC on behalf of International Union of Biochemistry and Molecular Biology.

KEYWORDS

ARES, ARF7, AUXIN, lateral root development, long noncoding RNA, SOLITARYROOT

1 | INTRODUCTION

During the last few years, plant long noncoding RNAs (lncRNAs) have been linked to a wide variety of molecular mechanisms modulating gene expression, ranging from epigenetics and transcription, to translation and protein modification.¹ Nuclear-enriched lncRNAs regulate gene expression through diverse mechanisms, including epigenetics, splicing, and subcellular localization of protein partners.^{1,2} Some lncRNAs act in *cis*, by recruiting histone-modifying complexes,^{3,4} by RNA Polymerase II (Pol II) collision of convergent genes,⁵ by influencing the stability or translation of its overlapping gene⁶ or by modulating chromatin 3D conformation.^{7,8} On the other hand, *trans*-acting lncRNAs may act through DNA–RNA or protein–RNA duplex formation for the regulation of gene expression.

The lncRNA *APOLO* is known to regulate its neighbor gene *PID* by dynamically modulating chromatin 3D conformation in response to auxin.⁷ Furthermore, *APOLO* is transcribed by Pol IV and V, and subjected to RNA-directed DNA methylation (RdDM), supporting that *APOLO* methylation status can affect its function on chromatin dynamics. More recently, it was shown that *APOLO* can recognize multiple independent loci across the Arabidopsis genome by sequence complementarity and R-loop formation. *APOLO* can modulate target chromatin conformation dynamics by interaction with Polycomb proteins⁹ and transcription factors.¹⁰ As a result, *APOLO* regulates auxin-responsive lateral root development and the expansion of root hair cells at low temperatures.

Here we browsed through the *Arabidopsis thaliana* genome in search of *APOLO*-like lncRNAs to assess if they perform *cis* and/or *trans* actions. To this end, we looked for loci transcribed into lncRNAs in Arabidopsis roots, as previously identified.¹¹ We focused on precursors of 24 nt siRNAs, that is, controlled by RdDM. Finally, we selected those whose neighbors are known players in root development. After analyzing the co-transcriptional accumulation of adjacent genes along Arabidopsis development, we chose a novel lncRNA for further characterization. The *AUXIN REGULATOR ELEMENT DOWNSTREAM SOLITARYROOT* (*ARES*) is encoded downstream of the lateral root master regulator *IAA14/SLR*,¹² and both loci are regulated during LR development. However, *ARES* knockdown does not affect *IAA14* gene expression although these plants exhibit a lateral root developmental disorder, in agreement with the transcriptomic analysis uncovering deregulated genes.

Altogether, our study hints at *ARES* as a *trans*-acting lncRNA participating in lateral root development.

2 | RESULTS

2.1 | The locus *ARES* is regulated by RdDM and is transcribed into a nuclear-enriched long noncoding RNA co-regulated with its neighbor gene *SOLITARYROOT*

Among the 1,671 intergenic lncRNAs (or lincRNAs) detected in *Arabidopsis thaliana* root tips,¹¹ 456 co-localize with 24 nt siRNAs (Table S1¹¹), potentially regulated through RdDM and affecting the activity of neighboring genes. Interestingly, five lincRNAs/siRNA precursors are neighbors to root-related coding genes (Tables S1 and S2, shortlist derived from the literature¹³): *XLOC_005697*, *XLOC_002421*, *AT1G48625*, *AT2G34655* (*APOLO* lncRNA), and *AT4G14548/ARES* (Figure 1a). Using the Genevestigator database,¹⁴ we explored the expression of the shortlisted lincRNAs and their respective neighbor coding genes in roots, and their potential co-regulation during plant development. *XLOC_005697* and *XLOC_002421* are not included in the official Arabidopsis annotations and thus were not available in this database. The lncRNA encoded by *AT1G48625* was only detected in inflorescences, thus poorly correlated with its neighbor gene *AT1G48630/RACK1B* which is expressed ubiquitously during plant development (Figure S1). Interestingly, the lncRNA *ARES* and its closest neighbor gene *AT5G14550 (IAA14/SLR)* are detected in roots and expressed throughout the life of the plant and to a lesser extent in reproductive-related organs, including flower primordium, flower, siliques, and seeds (Figure 1b,c). Furthermore, analysis of publicly available transcriptomic datasets (TraVa) revealed that the *ARES* lncRNA transcriptional accumulation significantly and positively correlates with that of its coding neighboring genes, that is, *NF-YB3* and *IAA14* (Figure 1d; *AT4G06195* is not included in the TraVa database). Considering this lncRNA is positioned very close to *IAA14*, we called it *ARES*.

To further confirm that the lncRNA *ARES* is regulated through RdDM, we measured its expression in mutant plants altered in this process. As expected, the expression of *ARES* was significantly higher in the *nrpd2a* (common subunit of Pol IV and V), *nrpd1a4* (subunit of Pol IV) and *dcl3* mutant lines, providing additional evidence that this locus is controlled by RdDM

(Figure S2). The poor coding capacity of the lincRNA *ARES* was confirmed by independent coding potential estimators, and compared to the already described *MARS* lncRNA⁴ (Figure 1e). In addition, we found that this transcript is accumulated in the cell nucleus (Figure 1f), hinting at a possible role in epigenetic regulations, chromatin action or alternative splicing.

2.2 | The lncRNA *ARES* regulates root growth

To determine whether the transcriptional activity of the *ARES* lncRNA may affect its neighbor genes in *cis*, we isolated homozygous lines of one SALK insertional mutant [*SALK 113294*; located prior *ARES* TSS^{15,16}

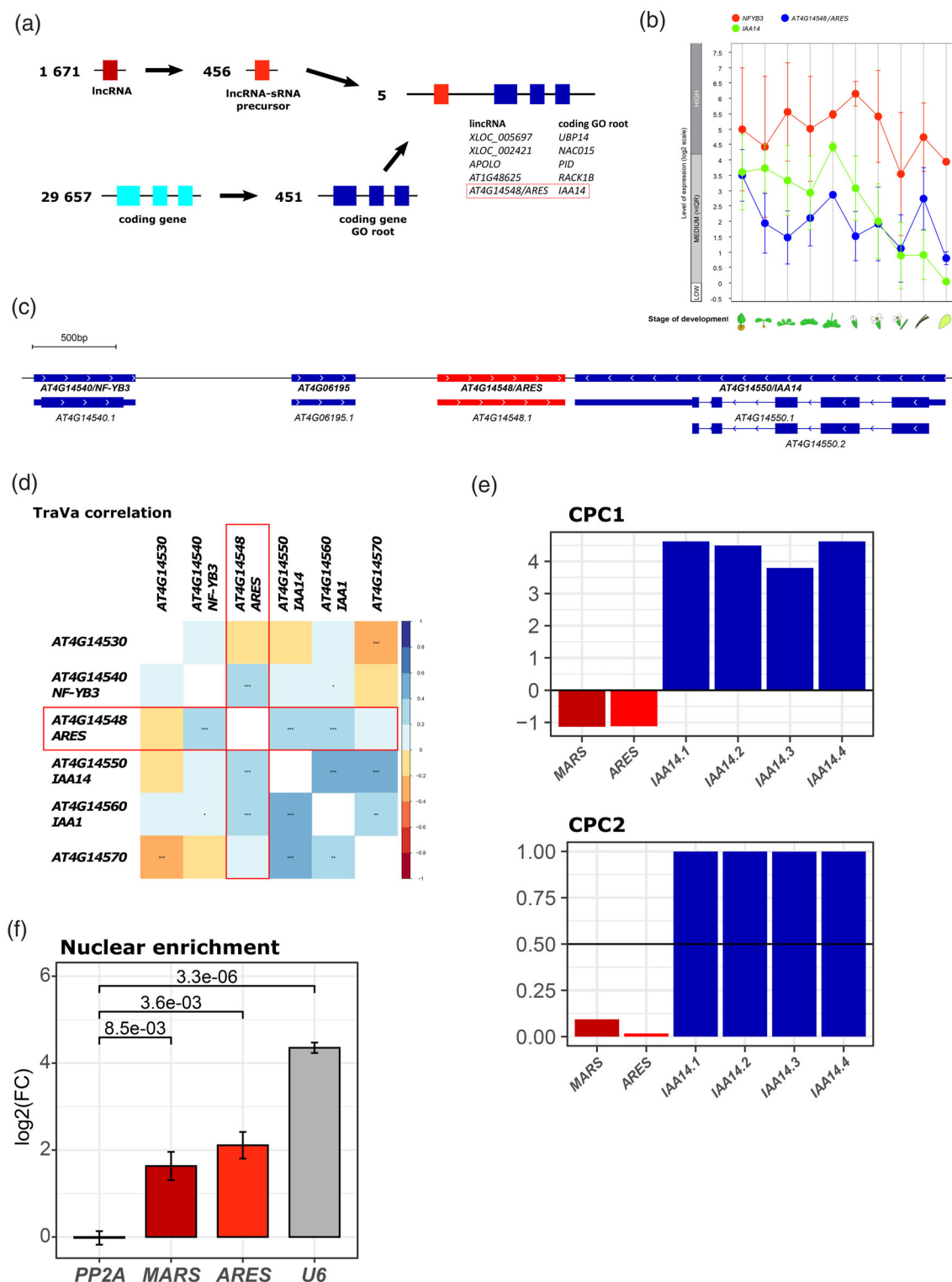


FIGURE 1 Legend on next page.

(Figure S3A)] and three independent knockdown lines by RNAi, targeting *ARES* 5' region (Figure S3A). *ARES* transcript abundance was reduced in all the lines as compared to Col0. Interestingly, Pol II binding was significantly reduced in the RNAi-*ARES* 3.2 as compared to Col0, suggesting that the RNAi constructs may have reduced the transcription of *ARES* lncRNA in addition to its post-transcriptional degradation (Figure S3B). Despite changes in *ARES* transcriptional activity upon silencing, none of these lines showed a deregulated expression of the two adjacent coding genes, *IAA14* nor of *NF-YB3*, in control conditions (Figure 2a). The expression of the neighboring lncRNA *AT4G06195* remains also unaffected upon *ARES* misregulation (Figure S3C). Considering the role of *IAA14* in auxin-dependent lateral root development, we also assessed the transcriptional response of *ARES* and its neighbor genes during a lateral root induction kinetics (NPA/NAA treatment¹⁷). Interestingly, both *IAA14* and *ARES* transcript abundance increased, reaching a maximum at 6 h of treatment, while *NF-YB3* transcript abundance decreases with the treatment (Figure 2b). Upon *ARES* knockdown, *IAA14* conserved the same expression level and pattern along the lateral root induction kinetics likewise for *IAA1*, a homolog gene encoded upstream of *IAA14*. Strikingly, *NF-YB3* was significantly up-regulated by the NPA treatment compared to WT but continued with the same level of expression and pattern as in WT in the other time points of the lateral root induction kinetics. Additionally, when plants were treated with NAA alone (without prior application of NPA), the transcript levels of *ARES*, *IAA14*, and *IAA1* were found to increase, whereas the transcript abundance of *NF-YB3* remained unchanged, in three out of four lines (Figure S4). The up-regulation observed only in the *ARES*-RNAi 6.2 lines may be due to the specific RNAi transgene insertion of this line. In agreement,

RNAi-*ARES* lines and the insertional mutant displayed similar responses to the treatment. Altogether, our results indicate that this noncoding transcript does not regulate *IAA14* in *cis*, but may have a direct or indirect effect on *NF-YB3* activity under NPA treatment.

Although *ARES* knockdown did not affect *IAA14* expression in our condition, their co-regulation in plant organs and NPA-NAA treatment (Figures 1d and 2b) made us wonder if this lncRNA may participate in lateral root development. Thus, we characterized root architecture in control conditions. Interestingly, while primary root length was unaffected, average lateral root length was slightly reduced in RNAi lines 1.2 and 3.2 and the insertional mutant, and significantly reduced in RNAi 6.2, the line showing one of the lowest levels of *ARES* (Figure 2c). In agreement, lateral root density was significantly affected in the insertional mutant with low levels of *ARES* (Figure 2c). Altogether, our results suggest that the auxin-responsive lncRNA *ARES* participates in lateral root development. Notably, *ARES*-related phenotypes were observed in control conditions, in which the transcriptional activity of its neighbor genes *IAA14* and *NF-YB3* remain unaffected (at least in whole roots, as harvested here), suggesting that *ARES* regulatory role may not be mediated by a mechanism occurring in *cis*.

2.3 | The root transcriptome of *ARES* knockdown plants uncovers a link to auxin response and lateral root development

To better understand the role of *ARES* in root development, we investigated the full transcriptome of roots of RNAi line 6.2 through RNA-Seq. 1,665 genes were differentially accumulated upon *ARES* knockdown compared to WT. Gene Ontology (GO) analyses hinted at genes encoding nuclear-enriched proteins (cellular components);

FIGURE 1 The *AUXIN REGULATOR ELEMENT DOWNSTREAM SOLITARYROOT (ARES)* locus is transcribed into a long intergenic noncoding RNA downstream of the *IAA14* gene. (a) Flowchart of identification of lncRNA-siRNA which are adjacent to root-related genes. lncRNAs co-localizing with 24 nt siRNA and the neighbor coding gene with a Gene Ontology (GO) related to root growth and development were collected using the Blein et al (2020)¹¹ transcriptomic analyses and the GO consortium,¹³ respectively. The lncRNAs-siRNA potential precursor neighbors to a root-related gene were shortlisted. The resulting five lncRNAs and the name of the neighboring gene are indicated on the right. (b) Transcript abundance of *ARES* and neighbors' genes throughout plant life. Genevestigator snapshot from the Development condition search tool.¹⁴ (c) IGV snapshot of the *ARES* locus and surrounding neighboring genes. For each gene, exons are indicated with rectangles and introns with solid lines. (d) Pearson correlation analysis derived from transcriptomics data from TraVa datasets. Correlations between two genes are indicated with scores ranging from -1 to +1 where -1 corresponds to a negative correlation and +1 a positive correlation. A color scale indicates the Pearson correlation score. Each correlation was tested for significant differences (* for $p \leq 0.05$, ** for $p \leq 0.01$, *** for $p \leq 0.001$). (e) Coding potential of the *ARES* transcript. Scores were determined using CPC1 and CPC2 (left to right) algorithms.^{45,46} For each analysis, the threshold between coding and noncoding genes is displayed with a horizontal dashed black line. Coding genes are situated above the threshold, whereas noncoding genes are situated under. *MARS* is used as positive control for noncoding transcripts. (f) Nuclear enrichment of *ARES*. The housekeeping transcript *PP2A* was considered as a negative control and U6 and the lncRNA *MARS* as positive controls of nuclear-enriched transcripts, for comparison.

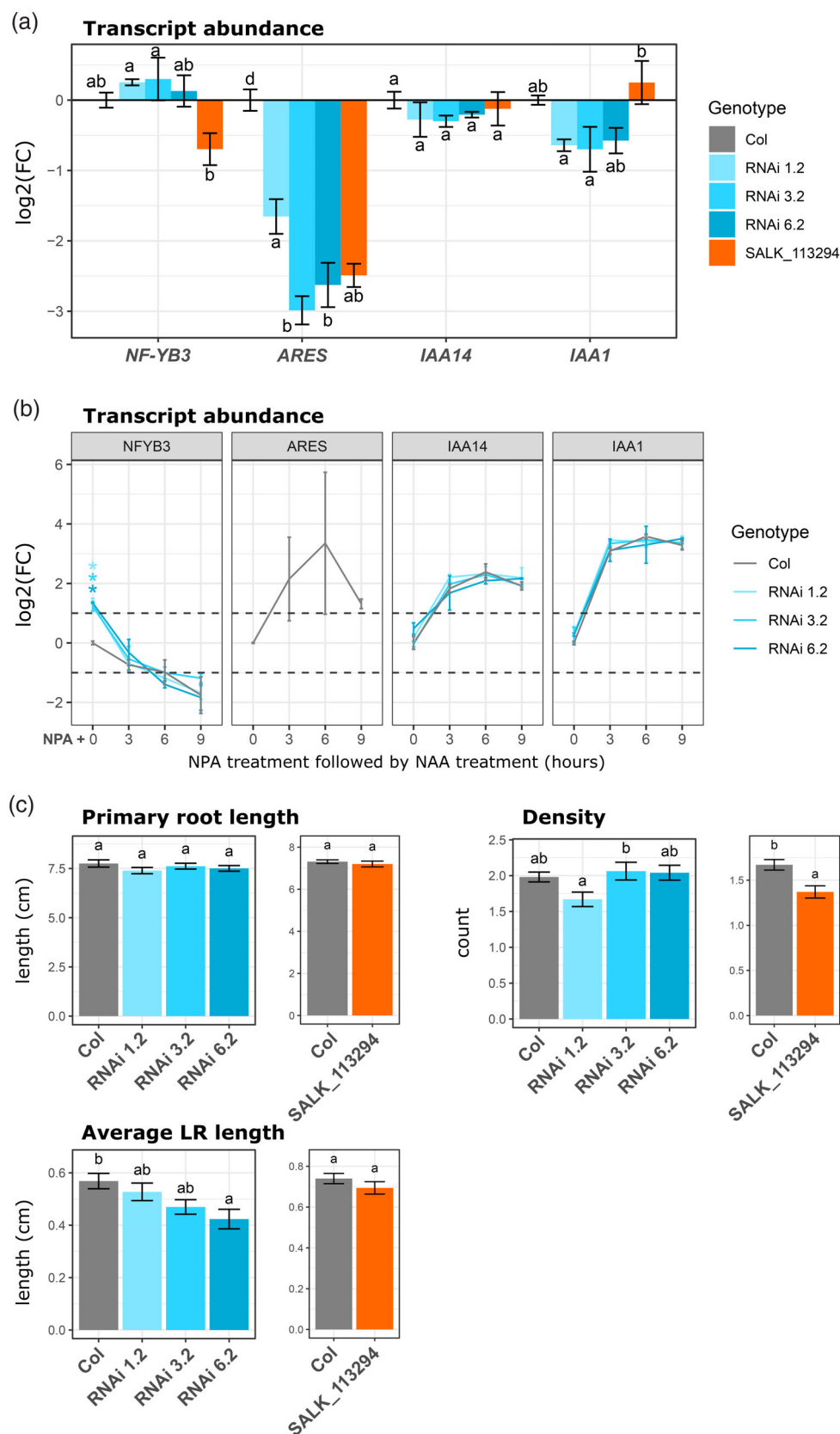


FIGURE 2 The knockdown and knockout of the lncRNA *AUXIN REGULATOR ELEMENT DOWNSTREAM SOLITARYROOT* (*ARES*) result in an altered root architecture without affecting the expression of *IAA14*.

(a) Transcript abundance of *ARES* and its surrounding genes in control conditions in RNAi lines targeting *ARES* and the insertional mutant *SALK_113294*. Transcriptional abundance is shown as the mean \pm standard error ($n = 3$) of the log₂ fold change compared to the Col0 genotype. Results were analyzed by one-way analysis of variance (ANOVA) followed by Tukey's post-hoc test. For each gene, different letters indicate statistical differences between genotypes ($p \leq 0.05$). (b) Transcript levels of *ARES* and its surrounding genes in response to NPA/NAA treatment in RNAi lines targeting *ARES*. Gene expression data are shown as the mean \pm standard error ($n = 3$) of the log₂ fold change compared to time 0 h. Results were analyzed by one-way analysis of variance (ANOVA) followed by Tukey's post-hoc test. Statistical differences between RNAi-*ARES* and Col-0 ($p \leq 0.05$) are indicated by stars (*) for each gene and time-point. (c) Mean primary root length, lateral root length, and lateral root density according to the genotype of 12-day-old seedlings. Results were analyzed by one-way analysis of variance (ANOVA) followed by Tukey's post-hoc test. For each genotype, different letters indicate statistical differences ($p \leq 0.05$) between root architecture parameters.

protein and DNA interacting proteins (molecular functions); and notably root development, among several responses to the environment (biological processes;

Figure 3a). Interestingly, isoform and splicing variation analyses revealed a change in isoforms and alternative 3' ends for known root-related genes upon *ARES*

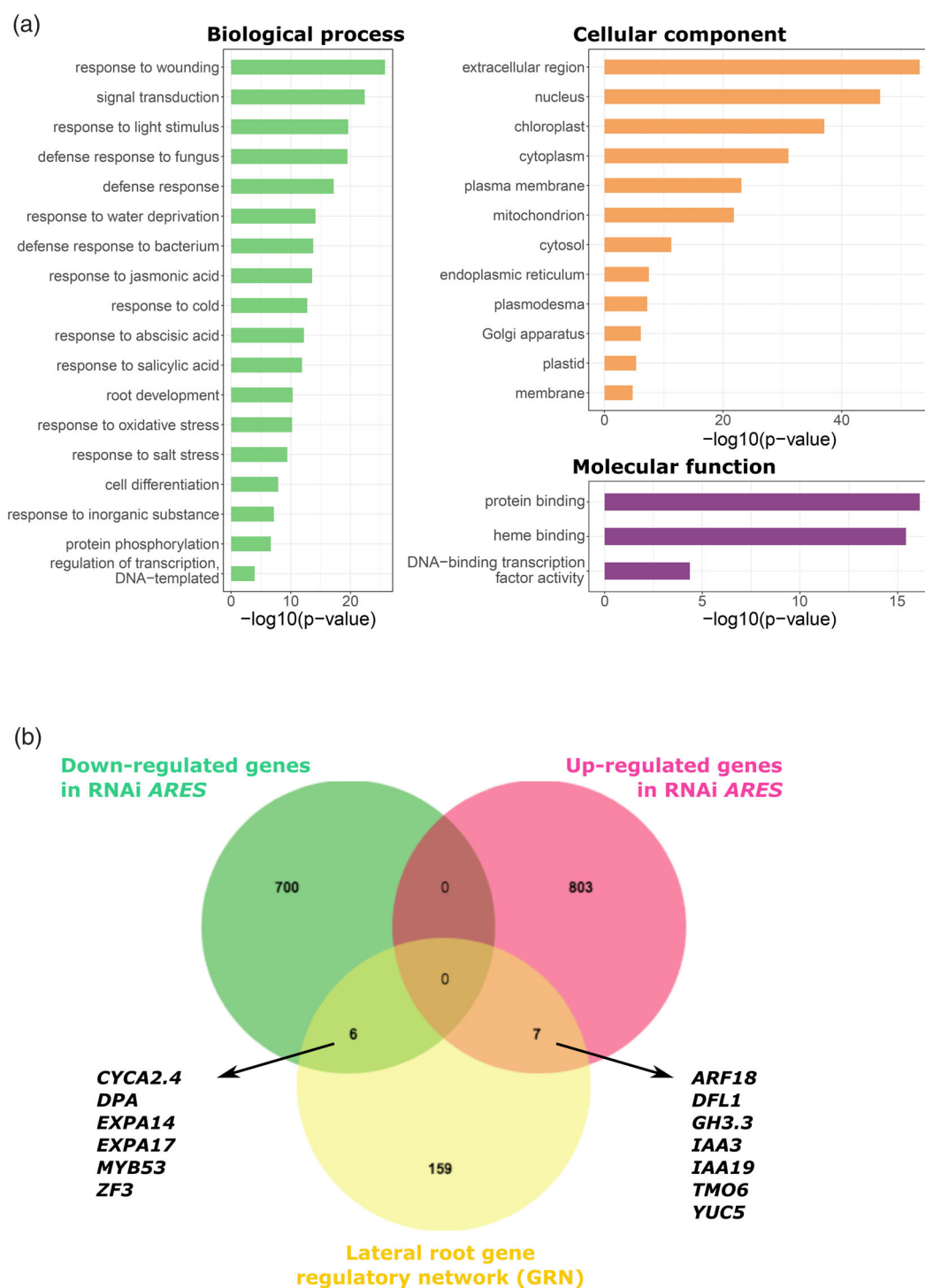


FIGURE 3 The lncRNA *AUXIN REGULATOR ELEMENT DOWNSTREAM SOLITARYROOT* (*ARES*) regulates auxin-responsive genes involved in lateral root development. (a) Significant enrichment of GO terms in RNAi-*ARES* DEGs for biological processes, cellular components, and molecular function. (b) Overlap between RNAi-*ARES* DEGs (up and down) and genes involved in the lateral root gene regulatory network.¹⁸

downregulation, including *PIP5K*, *HPA1*, and *HSP20-like*, respectively (Table S3). To further explore the role of *ARES* during lateral root development, we investigated the lateral root gene regulatory network (GRN) defined by Lavenus

et al.¹⁸ Among the 172 genes included in these GRN, 13 were deregulated in the RNAi-*ARES* 6.2 line: 6 were downregulated in RNAi-*ARES*, and 7 upregulated (Figure 3b), notably including well-known factors

participating in lateral root development, like *YUCCA5*,¹⁹ *IAA19*²⁰ and *SHY2/IAA3*,²¹ among others. Changes in transcript abundance were confirmed for seven out of eight of these genes in the three RNAi lines, supporting

that *ARES* may play a regulatory role in the expression of these root-related genes (Figure S5). Furthermore, when we compared the list of differentially expressed genes (DEG) with available datasets of auxin responses in

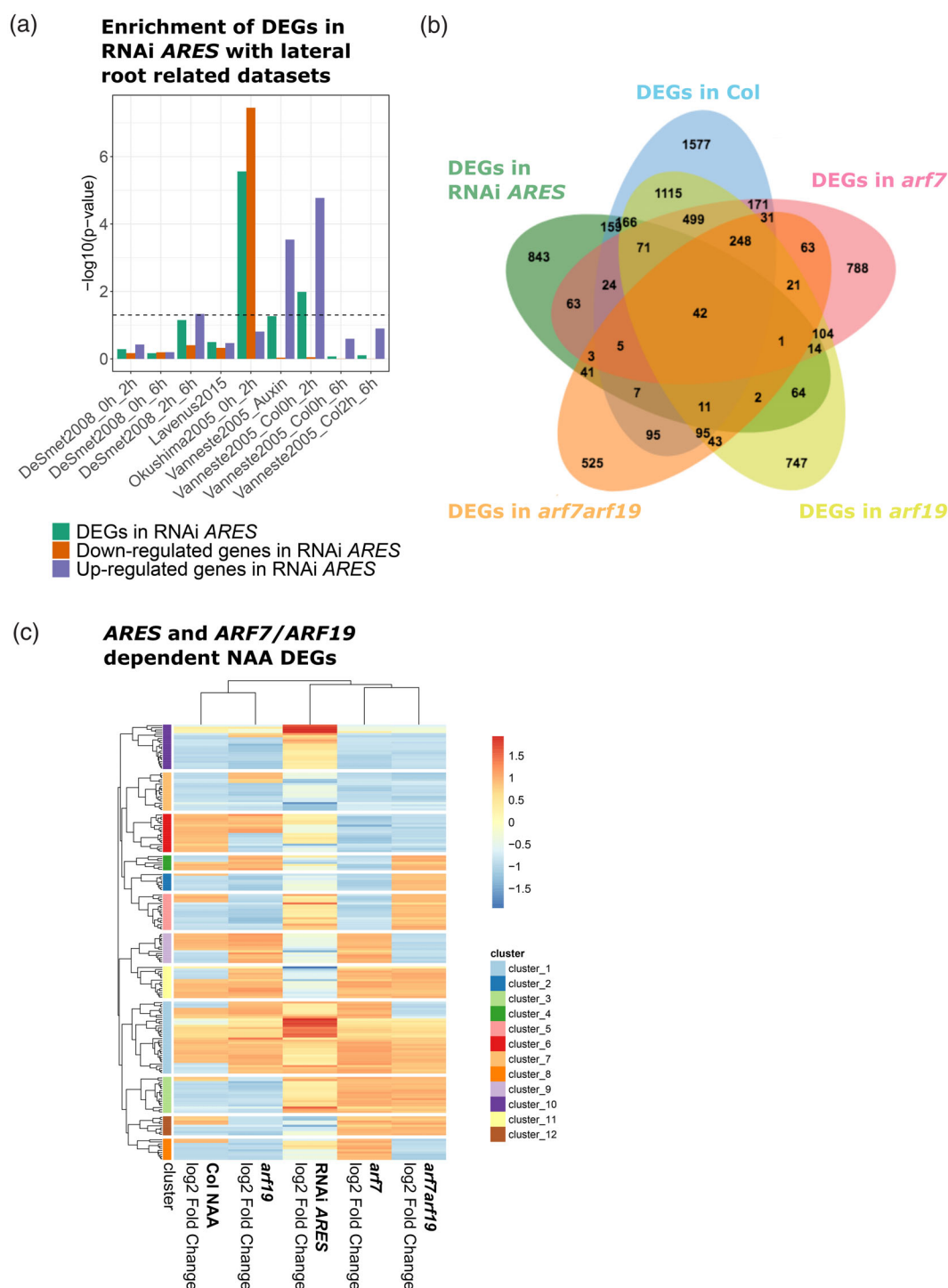


FIGURE 4 AUXIN REGULATOR ELEMENT DOWNSTREAM SOLITARYROOT (*ARES*)-regulated genes are mainly dependent on *ARF7* control in response to auxin. (a) Enrichment of RNAi-*ARES* DEGs (all, down and up) in gene list related to lateral root initiation and development.¹⁸ (b) Overlap between RNAi-*ARES* DEGs with auxin-responsive genes in Col0, *arf7*, *arf19*, *arf7 arf19*. (c) Hierarchical clustering of all RNAi-*ARES* DEGs that are *ARF7* or *ARF19* dependent responsive to auxin based on the scaled log2 fold change in RNAi-*ARES* and NAA treated Col0, *arf7*, *arf19*, *arf7 arf19*. Colors correspond to the scaled log2 fold change in each condition.

Arabidopsis roots, we found a strong enrichment of DEG after a 2 h NAA treatment, derived from two independent works (Figure 4a,^{22,23}). In the latest, DEG in response to auxin were particularly overlapped with upregulated genes in RNAi-*ARES* roots. A deeper analysis of the dataset published by Okushima and co-workers²⁴ allowed us to determine that 45.2% ($n = 488$) of *ARES*-deregulated genes are modulated in response to auxin in Col0, *arf7*, *arf9*, or *arf7-arf19* mutant, whereas 134 genes are dependent on *ARF7/ARF19* (Figure 4b).

Clustering analyses limited to the RNAi-*ARES* DEG, and *ARF7* and/or *ARF19*-dependent auxin-responsive genes (²⁴; see Table S4A for genes ID of each cluster), showed that RNAi-*ARES* transcriptome (in control conditions) groups together with *arf7* and *arf7 arf19* double mutant in response to auxin, whereas the profile of genes in *arf19* and WT form a separate group (Figure 4c and Figure S6). Our observations indicate that *ARES* participates in lateral root development in the regulatory pathways dependent on *ARF7*. Furthermore, the clustering analysis revealed that depending on the group of DEG, the link with the response to auxin differs. Cluster 3 groups genes, which behave similarly in RNAi-*ARES* in control conditions and in *arf7* and *arf7/19* roots in response to auxin, whereas these genes exhibit an opposite behavior in WT and *arf19* single mutants under auxin treatment. Cluster 5 group genes are induced in RNAi-*ARES* and *arf7/19* in response to auxin, in contrast to their activity in WT and both single *ARF* mutants. Clusters 10 and 11 group genes, which are induced or repressed upon *ARES* knockdown, respectively, in contrast to an *ARF*-independent response to auxin. Finally, cluster 12 is the only one grouping genes showing a closer behavior between WT, *arf19*, and RNAi-*ARES*, in contrast to *arf7* and *arf7/19*. Altogether, our observations suggest that *ARES* participates in auxin signaling during lateral root development. Altogether, our observations suggest that *ARES* participates in auxin signaling during lateral root development. Additionally, *ARES* downregulation also leads to changes in the splicing of certain genes important for root growth, and the expression of a significant number of auxin-responsive genes, some of which are dependent on *ARF7* and/or *ARF19*.

3 | DISCUSSION

Lateral root development relies largely on auxin homeostasis and the consequent signaling pathways.^{25,26} Among the key regulatory genes mediating the action of auxin, we find the TF family of Auxin Response Factors (ARFs) and their related Aux/IAA repressing partners. Twenty-nine Aux/IAA genes are annotated in Arabidopsis and

encode short-nuclear proteins involved in the inactivation of the ARF proteins, consequently repressing the auxin transcriptional responses. Auxin stimulus increases the interaction between Aux/IAA proteins and the Skp1-Cullin-F-box/Transport Inhibitor Response 1 (SCF-TIR1) complex, promoting the proteasome-mediated degradation of the Aux/IAA proteins. Notably, gain-of-function mutations of 10 IAA proteins affect plant development. Among them, *iaa14/slr* gain-of-function mutation stops the auxin-mediated cell division in the pericycle, blocking the development of lateral roots.^{22,23}

Here, we investigated the noncoding transcriptome of Arabidopsis roots¹¹ to search for *APOLO*-like RdDM-regulated lincRNAs, which are located next to critical root growth modulator genes, in order to assess if they participate in similar molecular mechanisms as the lincRNA *APOLO*.⁷ As a result, we focused on an uncharacterized lincRNA that we named *ARES* located downstream of the lateral root master regulator *IAA14*. Our data shows that *ARES* is regulated during lateral root formation and participates in the regulation of its development through the regulation of lateral root-related genes. Even though our data suggest that *ARES* acts in *trans* we cannot exclude that its function is entirely independent from its neighboring genes *NF-YB3* and/or *IAA14*, or other non-neighboring genes not known to regulate root growth.

Local activity of lincRNAs has been shown for *APOLO*,⁷ as well as for other lincRNAs. Recently, the lincRNA *MARS* was implicated in the modulation of the local chromatin conformation in response to ABA, fine-tuning the transcriptional activity of the marneral cluster of genes in Arabidopsis. Likewise *APOLO*, *MARS* directly interacts and titrates the Polycomb protein LHP1 across the region, fine-tuning the epigenetic pattern.⁴ However, it remains uncertain if *MARS* can also regulate other genes in *trans*. Several lincRNAs were shown to directly recruit Polycomb proteins, notably the histone methyltransferase CURLY LEAF (CLF), to their transcriptional site, affecting the expression of nearby genes.^{4,8,27,28} On the other hand, alternative lincRNAs were also shown to recruit different chromatin-related proteins triggering the deposition of active histone marks H3K4me3 and H4K16Ac in Arabidopsis or rice.^{29,30} Although *ARES* deregulation did not strongly affect the transcriptional activity of its adjacent gene *IAA14*, it upregulated the expression of *NF-YB3* under NPA treatment. It is unclear whether *NF-YB3*, which has been shown to enhance heat stress tolerance in plants,³¹ also plays a role in regulating lateral root growth, thus we cannot exclude that the *ARES*-mediated *NF-YB3* upregulation does not participate in the auxin-dependent lateral

root growth. Similarly, other genes not known to regulate root growth are deregulated upon *ARES* knockdown and may also participate in the root-related phenotype observed. Furthermore, it is worth noting that similarly to *MARS* and *APOLO*, *ARES* is co-regulated with its closest neighboring gene in response to stress, hinting at an interplay between coding and noncoding transcription and their nearby regulatory elements under stress conditions. In Arabidopsis roots, co- and anti-co-regulation of transcription between coding and noncoding neighboring loci were systematically observed for a subset of lncRNAs in response to phosphate starvation.¹¹ The regulation of neighbor genes by noncoding transcription was also described for the lncRNA *SVALKKA*.⁵ Pol II read-through transcription of *SVALKKA* results in a cryptic lncRNA overlapping the locus encoding the TF CBF1 on the antisense strand, termed as *CBF1*. *CBF1* transcription is suppressed by Pol II collision with the *SVALKKA-asCBF1* lncRNA.

Although convergent transcription may have led to Pol II collision between *ARES* and *IAA14*, no overlap has been observed between the two loci (Figure S3), and notably the knockdown of *ARES* does not affect *IAA14* transcriptional activity. Even though CAGE-seq data indicated an absence of overlap between *ARES* and *IAA14* (Figure S3), further experiments should be performed to confirm it, notably in response to auxin. It is of importance as auxin directly affects polyadenylation site usage of *IAA14* and is crucial for downstream regulation of *ARF7* and *ARF19*.³² Furthermore, as *IAA14* and *ARES* do not seem to overlap, their RNAs should not form natural antisense transcript (NAT) pairs, which may have eventually led to the translational promotion of *IAA14* like shown for *PHO1;2* and its cognate NAT in rice. The NAT expression promotes the shuttle of the sense-antisense RNA pair towards polysomes.⁶

Other nuclear-enriched lncRNAs have been identified as *trans*-regulatory transcripts. The lncRNA *ASCO* modulates alternative splicing by interacting with several splicing factors, including NSRa/b, PRP8a, and SmD1b. However, the physical interaction between *ASCO* and genes subjected to alternative splicing has not been explored. Notably, the deregulation of *ASCO* and its partners leads to root developmental phenotypes.²⁶ The lncRNA *HID1* also regulates its target gene *PIF3* in *trans*. *HID1* participates in large ribonucleoprotein complexes whose composition remains unknown, although it has been shown that *HID1* triggers transcriptional repression of *PIF3*.³³ In Arabidopsis, the TE-derived *lincRNA11195* mediates sensitivity to ABA as demonstrated by longer roots and higher shoot biomass in mutant plants when compared to wild-type. However, the molecular basis behind the action of *lincRNA11195* remains unknown.³⁴

Here we identified *ARES* for its similarity with *APOLO* profile, that is, (i) an intergenic lncRNA, (ii) precursor of 24 nt siRNAs, and (iii) neighbor of a root-related gene. Interestingly, in contrast to *APOLO*, *ARES* does not seem to regulate its adjacent locus, even though we cannot entirely exclude this possibility notably at the post-transcriptional or translational level. One major difference between *APOLO* and *ARES* is that the former and its neighbor gene *PID* are divergent and they likely share a single promoter encompassed in the intergenic region. In contrast, *ARES* is located downstream *IAA14*, likely not interfering with the *IAA14* promoter. *ARES* vicinity to *IAA14* led us to assess root development in *ARES* knockdown plants (i.e., lines and one insertional mutant). *ARES* knockdown results in lateral root developmental alterations in agreement with the transcriptomic output revealed by RNA-Seq. Our *ARES*-mediated lateral root phenotype, although subtle, is characteristic of many lncRNA modes of action, which adjust gene expression levels rather than completely knocking them out.¹ While only RNAi 6.2 shows a statistically significant decrease in the lateral root length, all lines with reduced levels of *ARES* tend to have shorter lateral roots. Hence, the downregulation of *ARES* fine-tunes key root-related gene expression, resulting in subtle changes in lateral root growth. In particular, DEG in RNAi-*ARES* roots is enriched in auxin-responsive genes, notably including a large subset of genes exhibiting an opposite behavior to their response to exogenous auxin in wild-type plants. In addition, we observed significant changes in the proportions of isoforms of genes that are directly involved in the regulation of root growth, further supporting the role of *ARES* in regulating root growth. Moreover, by comparing RNAi-*ARES* transcriptome to the transcriptional datasets revealing the response to auxin in *arf7* and *arf19* mutants, we found that *ARES* may participate in *ARF7*-dependent pathways. Interestingly, *IAA14* functions through its interaction with *ARF7* and *ARF19*, notably the stability of the *IAA14* protein, rather than its transcript, plays a role in controlling *ARF7/19*-dependent auxin response. *Solitaryroot* gain of function mutant plants, with increased stability of *IAA14*, prevent auxin-dependent release of *ARF7/19* and blocked LR formation. Thus, one possibility is that the decreased root density in *ARES*-knockdown lines is due to a change in *IAA14* protein stability, likely influencing its interaction with *ARF7/19* and the resulting root architecture. Therefore, we propose that *ARES* participates in the intricate regulatory network behind the lateral root development event, likely by direct recognition of target loci in *trans*, or alternatively by modulating the action of protein partners in the cell nucleus, such as proteins involved in epigenetic regulation, chromatin accessibility or splicing.

4 | METHODS

4.1 | Screening for *ARES* identification

Coding, lncRNA, and siRNA annotations were collected according to Blein et al (2020)¹¹ transcriptomics dataset. The root-related GO was collected from the GO consortium¹³ and included all the GO terms related to root growth and development (see GO term and identifier in Table S2). *bedtools closest* to default parameter was used to identify the lncRNA-siRNA precursor close to a root-related gene.³⁵

4.2 | Plant lines generated and used for this study

All plants used in this study are in Columbia-0 background. RNAi lines of *ARES* were obtained using the pFRN binary vector³⁶ bearing 250 bp of the 5' exon of *ARES* gene (see primers in Table S5), initially sub-cloned into the pENTR™/D-TOPO™ vector system from Invitrogen™. Arabidopsis plants were transformed using *Agrobacterium tumefaciens* Agl-0.³⁷ The T-DNA inserted line *SALK_113294* was provided by the Nottingham Arabidopsis Stock Center (NASC). Homozygous mutants were identified by Polymerase Chain Reaction (PCR) (see primers in Table S5).

4.3 | Growth conditions and phenotypic analyses

For single time-point phenotyping, seeds were sown in plates vertically placed in a growing chamber in long-day conditions (16 h in light 150μE; 8 h in dark; 21°C). Plants were grown on solid half-strength MS medium (MS/2) supplemented with 0.7% sucrose and supplemented with 0.8 g/L agar (Sigma-Aldrich, A1296 #BCBL6182V), buffered at pH 5.6 with 3.4 mM 2-(N-morpholino) ethane sulfonic acid. For root phenotype characterization, the root length was measured at 12 days after sowing (DAS) using RootNav software³⁸ from images taken with a flat scanner. For the lateral root induction time series, 7 days old seedlings were grown in MS/2 on nylon membranes and transferred to plates containing MS/2 containing 10 μM 1-N-Naphthylphthalamic acid (NPA), an inhibitor of auxin transport and lateral root development,¹⁷ for 3 days and transferred to MS/2 plates containing synthetic auxin (1-Naphthaleneacetic acid NAA) at 10 μM to induce lateral root development. Roots were sampled after 0, 3, 6, and 9 h of NAA treatment. For the NAA

treatment, seedlings were sprayed with 10 μM at 12 DAS and collected before and 24 h after the treatment.

4.4 | RT-qPCR

Total RNA was extracted from roots using TRI Reagent™ (Sigma-Aldrich) and treated with DNase (Fermentas) as indicated by the manufacturers. Reverse transcription was performed using 1 μg total RNA and the Maxima Reverse Transcriptase (Thermo Scientific) with oligo-dT primers. qPCR was performed on a Light Cyclor 480 with SYBR Green master I (Roche) in standard protocol (40 cycles, 60°C annealing). Primers used in this study are listed in Table S5 and depicted in Figure S3 for *ARES* and *IAA14*. Data were analyzed using the $\Delta\Delta C_t$ method using *PROTEIN PHOSPHATASE 2A SUBUNIT A3* (*AT1G13320*) for gene normalization³⁹ and time 0 for time-course experiments.

4.5 | Nuclear purification

WT seedlings were collected to assess the subcellular localization of RNAs. Chromatin was extracted as previously described.⁷ Briefly, 1 g of 12DAS non-crosslinked tissue was smashed to powder in liquid nitrogen and resuspended in 25 mL of EB1 (10 mM Tris pH 8, 0.4 M sucrose, 10 mM MgCl₂, 5 mM BME, 0.2 mM PMSF, 1X RNase inhibitor SIGMA R7397). After 5 min incubation on ice, samples were filtered two times in 70μm Falcon cell strainer (Fisher, 352,350). 200 μL of the solution was collected and mixed with 800 μL of TRI Reagent (Sigma-Aldrich) and corresponds to the 'total RNA fraction'. Filtered samples were then centrifuged for 20 min at 2,000 g and 4°C. Pellets were resuspended in 10 mL of EB2 (10 mM Tris pH 8, 0.25 M sucrose, 10 mM MgCl₂, 5 mM BME, 1% Triton X100, 100 μM PMSF, 1X RNase inhibitor SIGMA R7397) and centrifuged for 10 min at 2,000 g and 4°C. Finally, a sucrose gradient using 600–600 μL of EB3 (10 mM Tris pH 8, 1.7 M sucrose, 2 mM MgCl₂, 5 mM BME, 0.15% Triton X100) and EB3 re-suspended samples was performed to purify the chromatin. Purified chromatin was resuspended in 1 mL of TRI Reagent (Sigma-Aldrich) and corresponds to the 'nuclear RNA fraction'. RNA samples were treated with DNase, and reverse transcription was performed using random hexamers prior to qPCR analysis. Data were analyzed using the $\Delta\Delta C_t$ method using *PROTEIN PHOSPHATASE 2A SUBUNIT A3* (*AT1G13320*) for gene normalization³⁹ and the total fraction to assess nuclear enrichment.

4.6 | ChIP pol II

Chromatin immunoprecipitation (ChIP) assays were performed on 12-day-old seedlings using anti-IgG (Cell Signaling 2,729) and Pol II (Abcam ab817) antibodies, as described in Ariel et al (2020).⁹ Briefly, 1% formaldehyde crosslinked chromatin was resuspended in a solution containing 10 mM Tris-HCl pH 8, 0.4 M sucrose, 10 mM MgCl₂, 5 mM βME, and RNase. After centrifugation, the cell membrane was lysed in a solution containing 10 mM Tris-HCl pH 8, 0.25 M sucrose, 10 mM MgCl₂, 5 mM βME, 1% TRITON X100, and 200 μM PMSF. The chromatin was then placed on a sucrose gradient made with a lower layer of pure buffer (10 mM Tris-HCl pH 8, 1.7 M sucrose, 2 mM MgCl₂, 5 mM βME, and 0.15% TRITON X100) and an upper layer of resuspended pellet in the same buffer. The nuclei were resuspended in 300 μL of Nuclei Lysis Buffer (50 mM Tris-HCl pH 8, 0.1% SDS, 10 mM EDTA, and 1 μL of 20 U/μL RNAase-in Promega per sample) and sonicated using a water bath Bioruptor Pico (Diagenode; 30 s on/ 30 s off pulses, at high intensity for 10 cycles). ChIP was performed using Invitrogen Protein A Dynabeads. The immunoprecipitated DNA was recovered using Phenol:Chloroform:Isoamyl Alcohol (25:24:1; Sigma) and analyzed by qPCR. An untreated sonicated chromatin was processed in parallel and considered the Input sample.

4.7 | Library construction and sequencing

Three biological replicates of 12 DAS whole roots grown in control conditions were collected. RNA samples were extracted using TRI Reagent (Sigma-Aldrich) and treated with DNase (Fermentas) as indicated by the manufacturers. Libraries were processed using Illumina Stranded mRNA Prep library preparation kit following the manufacturer's instructions, starting with one microgram of total RNA. 2 × 75-nt paired-end reads were sequenced on a NextSeq 500 Sequencing System (Illumina). Sequence files generated in this study have been deposited in the NCBI GEO database under the accession GSE207358.

4.8 | Differential expression analysis and clustering

Adapter and poor-quality sequences were trimmed using Trimmomatic and ribosomal sequences were removed using sortMeRNA.⁴⁰ Cleaned mRNA reads were aligned on the TAIR10 genome⁴¹ using STAR (version 2.7.2a⁴²)

with the following arguments: --alignIntronMin 20--alignIntronMax 3,000--outSAMtype BAM SortedByCoordinate. Read overlapping exons were counted per genes using featureCounts from the subread package (v1.6.5,⁴³) using strand-specific mode (-s 2 -O -M--fraction). Differential gene expression and GO analysis were performed by edgeR using the DicoExpress package⁴⁴ using a linear model with genotype and replicate as explanatory factors. Genes with less than 1 count per million reads (CPM) were filtered out as low counts and raw *p*-values were adjusted with Benjamini & Hochberg method (FDR). Differentially expressed genes were defined as having an adjusted *p*-value lower than 0.05. GO enrichment analysis of DEG was conducted with DicoExpress Enrichment module.

To be able to compare the expression modification induced by *ARES* downregulation (RNA-seq) with the influence of auxin on Col0, *arf7*, *arf19*, and *arf7 arf19*, we used log2 fold change value that we scale per gene. The clustering of the genes and the samples was done using the Euclidean distance between genes and using hierarchical clustering. The number of clusters was determined manually.

4.9 | Bioinformatic analyses of transcriptomic datasets

Coding potential was calculated according to CPC1⁴⁵ and CPC2⁴⁶ methods. Enrichment with LR-related datasets was done by comparing the list of differentially expressed genes in RNAi-*ARES* (down and up) versus the different lists of differentially expressed genes present in the VisuaLRTC. Statistical enrichment was conducted with a hypergeometric test.^{18,23,24,47} Only genes present on the ATH1 Affymetrix were kept for the enrichment analysis. Venn diagrams were drawn with jvenn.⁴⁸

Splicing analysis was performed using SUPPA software (version 2.3,⁴⁹) using AtRTD3 annotation.⁵⁰ Transcript accumulation was estimated using kallisto (version 0.46.1,⁵¹) with the following arguments -b 100--rf-stranded. Isoform and splicing event quantification and comparison were processed according to SUPPA's manual and the *p*-value was corrected using FDR.

FUNDING INFORMATION

Saclay Plant Sciences-SPS (ANR-17-EUR-0007) to T.R., A.B., M.C. and T.B.; ICGB CRP-ARG01 and PICT 2019-4137 (Agence I+D+i) to F.A.; CNRS (Laboratoire International Associé NOCOSYM) to M.C. and F.A.; ECOSUD (no. A20N05) to T.B. and F.A. T.R. and A.B. were awarded a PhD scholarship from the French "Ministère de l'Enseignement supérieur, de la Recherche et de

l'Innovation". F.A. is a researcher from CONICET, and F.L. and A.B. are PhD fellows from the same institution.

CONFLICT OF INTEREST STATEMENT

No conflict of interest declared by authors.

ORCID

Thomas Roulé  <https://orcid.org/0000-0001-6661-9357>

Nicolás Gaggion  <https://orcid.org/0000-0002-6684-5300>

Martin Crespi  <https://orcid.org/0000-0002-5698-9482>

Federico Ariel  <https://orcid.org/0000-0001-8478-8808>

Thomas Blein  <https://orcid.org/0000-0001-9788-5201>

REFERENCES

- Lucero L, Fonouni-Farde C, Crespi M, Ariel F. Long noncoding RNAs shape transcription in plants. *Transcription*. 2020; 11(3-4):160–171.
- Romero-Barrios N, Legascue MF, Benhamed M, Ariel F, Crespi M. Survey and summary splicing regulation by long noncoding RNAs. *Nucleic Acids Res*. 2018;46(5):2169–2184.
- Fonouni-Farde C, Ariel F, Crespi M. Plant long noncoding rnas: New players in the field of post-transcriptional regulations. *Noncoding RNA*. 2021;7(1):1–17.
- Roulé T, Christ A, Hussain N, et al. The lncRNA MARS modulates the epigenetic reprogramming of the maternal cluster in response to ABA. *Mol Plant*. 2022;15:840–856.
- Kindgren P, Ard R, Ivanov M, Marquardt S. Transcriptional read-through of the long non-coding RNA SVALKA governs plant cold acclimation. *Nat Commun*. 2018;9(1):4561.
- Jabnune M, Secco D, Lecampion C, Robaglia C, Shu Q, Poirier Y. A Rice cis-natural antisense RNA acts as a translational enhancer for its cognate mRNA and contributes to phosphate homeostasis and plant fitness. *Plant Cell*. 2013;25(10):4166–4182.
- Ariel F, Jegu T, Latrasse D, et al. Noncoding transcription by alternative rna polymerases dynamically regulates an auxin-driven chromatin loop. *Mol Cell*. 2014;55(3):383–396.
- Kim DH, Sung S. Vernalization-triggered intragenic chromatin-loop formation by long noncoding RNAs. *Dev Cell*. 2017;176(1):100–106.
- Ariel F, Lucero L, Christ A, et al. R-loop mediated trans action of the APOLO long noncoding RNA. *Mol Cell*. 2020;77(5):1055–1065.e4.
- Moison M, Pacheco JM, Lucero L, et al. The lncRNA APOLO interacts with the transcription factor WRKY42 to trigger root hair cell expansion in response to cold. *Mol Plant*. 2021;14(6):937–948.
- Blein T, Balzergue C, Roulé T, et al. Landscape of the non-coding transcriptome response of two Arabidopsis ecotypes to phosphate starvation. *Plant Physiol*. 2020;183:1058–1072.
- Fukaki H, Tameda S, Masuda H, Tasaka M. Lateral root formation is blocked by a gain-of-function mutation in the solitary-root/IAA14 gene of Arabidopsis. *Plant J*. 2002;29(2):153–168.
- Berardini TZ, Mundodi S, Reiser L, et al. Functional annotation of the Arabidopsis genome using controlled vocabularies. *Plant Physiol*. 2004;135(2):745–755.
- Hruz T, Laule O, Szabo G, et al. Genevestigator V3: A reference expression database for the meta-analysis of transcriptomes. *Adv Bioinform*. 2008;2008:1–5.
- Nielsen M, Ard R, Leng X, et al. Transcription-driven chromatin repression of Intragenic transcription start sites. *PLoS Genet*. 2019;15(2):e1007969. <https://doi.org/10.1371/journal.pgen.1007969>.
- Thieffry A, Vigh ML, Bornholdt J, Ivanov M, Brodersen P, Sandelin A. Characterization of arabidopsis thaliana promoter bidirectionality and antisense RNAs by inactivation of nuclear RNA decay pathways. *Plant Cell*. 2020;32(6):1845–1867.
- Himanen K, Boucheron E, Vanneste S, Engler JDA, Inzé D, Beeckman T. Auxin-mediated cell cycle activation during early lateral root initiation. *Planta*. 2002;14:2339–2351.
- Lavenus J, Goh T, Guyomarch S, et al. Inference of the arabidopsis lateral root gene regulatory network suggests a bifurcation mechanism that defines primordia flanking and central zones. *Plant Cell*. 2015;27(5):1368–1388.
- Jia Z, Giehl RFH, von Wirén N. Local auxin biosynthesis acts downstream of brassinosteroids to trigger root foraging for nitrogen. *Nat Commun*. 2021;12(1):5437.
- Zhang S, Yu R, Yu D, et al. The calcium signaling module CaM-IQM destabilizes IAA-ARF interaction to regulate callus and lateral root formation. *Proc Natl Acad Sci USA*. 2022;119:e2202669119.
- Goh T, Kasahara H, Mimura T, Kamiya Y, Fukaki H. Multiple AUX/IAA-ARF modules regulate lateral root formation: The role of Arabidopsis SHY2/IAA3-mediated auxin signalling. *Philos Transact R Soc B: Biol Sci*. 2012;367(1595):1461–1468.
- Fukaki H, Nakao Y, Okushima Y, Theologis A, Tasaka M. Tissue-specific expression of stabilized SOLITARY-ROOT/IAA14 alters lateral root development in Arabidopsis. *Plant J*. 2005; 44(3):382–395.
- Vanneste S, de Rybel B, Beemster GTS, et al. Cell cycle progression in the pericycle is not sufficient for SOLITARY ROOT/IAA14-mediated lateral root initiation in Arabidopsis thaliana. *Plant Cell*. 2005;17(11):3035–3050.
- Okushima Y, Overvoorde PJ, Arima K, et al. Functional genomic analysis of the AUXIN RESPONSE FACTOR gene family members in Arabidopsis thaliana: Unique and overlapping functions of ARF7 and ARF19. *Plant Cell*. 2005;17(2):444–463.
- Du Y, Scheres B. Lateral root formation and the multiple roles of auxin. *J Exp Bot*. 2018;69(2):155–167.
- Roulé T, Crespi M, Blein T. Regulatory long non-coding RNAs in root growth and development. *Biochem Soc Trans*. 2021;50:403–412.
- Heo JB, Sung S. Vernalization-mediated epigenetic silencing by a long intronic noncoding RNA. *Science*. 2011;331(6013):76–79.
- Wu HW, Deng S, Xu H, et al. A noncoding RNA transcribed from the AGAMOUS (AG) second intron binds to CURLY LEAF and represses AG expression in leaves. *New Phytol*. 2018;219(4):1480–1491.
- Wang Y, Luo X, Sun F, et al. Overexpressing lncRNA LAIR increases grain yield and regulates neighbouring gene cluster expression in rice. *Nat Commun*. 2018;9(1):1–9.
- Zhao X, Li J, Lian B, Gu H, Li Y, Qi Y. Global identification of Arabidopsis lncRNAs reveals the regulation of MAF4 by a natural antisense RNA. *Nat Commun*. 2018;9(1):1–12.
- Sato H, Suzuki T, Takahashi F, Shinozaki K, Yamaguchi-Shinozaki K. NF-YB2 and NF-YB3 have functionally diverged and differentially induce drought and heat stress-specific genes. *Plant Physiol*. 2019;180(3):1677–1690.

32. Hong L, Ye C, Lin J, Fu H, Wu X, Li QQ. Alternative polyadenylation is involved in auxin-based plant growth and development. *Plant J*. 2018;93(2):246–258.
33. Wang Y, Fan X, Lin F, et al. Arabidopsis noncoding RNA mediates control of photomorphogenesis by red light. *Proc Natl Acad Sci USA*. 2014;111(28):10359–10364.
34. Wang D, Qu Z, Yang L, et al. Transposable elements (TEs) contribute to stress-related long intergenic noncoding RNAs in plants. *Plant J*. 2017;90(1):133–146.
35. Quinlan AR, Hall IM. BEDTools: A flexible suite of utilities for comparing genomic features. *Bioinformatics*. 2010;26(6):841–842.
36. Ariel F, Brault-Hernandez M, Laffont C, et al. Two direct targets of cytokinin signaling regulate symbiotic nodulation in medicago truncatula. *Plant Cell*. 2012;24(9):3838–3852.
37. Clough SJ, Bent AF. Floral dip: A simplified method for agrobacterium-mediated transformation of Arabidopsis thaliana. *Plant J*. 1998;16(6):735–743.
38. Pound MP, French AP, Atkinson JA, Wells DM, Bennett MJ, Pridmore T. RootNav: Navigating images of complex root architectures. *Plant Physiol*. 2013;162(4):1802–1814.
39. Czechowski T, Stitt M, Altmann T, Udvardi MK, Scheible W-R. Genome-wide identification and testing of superior reference genes for transcript normalization in Arabidopsis. *Plant Physiol*. 2005;139:5–17.
40. Kopylova E, Noé L, Touzet H. SortMeRNA: Fast and accurate filtering of ribosomal RNAs in metatranscriptomic data. *Bioinformatics*. 2012;28(24):3211–3217.
41. Lamesch P, Berardini TZ, Li D, et al. The Arabidopsis Information resource (TAIR): Improved gene annotation and new tools. *Nucleic Acids Res*. 2012;40(D1):1202–1210.
42. Dobin A, Davis CA, Schlesinger F, et al. STAR: Ultrafast universal RNA-seq aligner. *Bioinformatics*. 2013;29(1):15–21.
43. Liao Y, Smyth GK, Shi W. FeatureCounts: An efficient general purpose program for assigning sequence reads to genomic features. *Bioinformatics*. 2014;30(7):923–930.
44. Lambert I, Paysant-Le Roux C, Colella S, Martin-Magniette ML. DiCoExpress: A tool to process multifactorial RNAseq experiments from quality controls to co-expression analysis through differential analysis based on contrasts inside GLM models. *Plant Methods*. 2020;16(1):68.
45. Kong L, Zhang Y, Ye ZQ, et al. CPC: Assess the protein-coding potential of transcripts using sequence features and support vector machine. *Nucleic Acids Res*. 2007;35(Suppl 2):345–349.
46. Kang YJ, Yang DC, Kong L, et al. CPC2: A fast and accurate coding potential calculator based on sequence intrinsic features. *Nucleic Acids Res*. 2017;45(W1):W12–W16.
47. Parizot B, de Rybel B, Beeckman T. VisuaLRTC: A new view on lateral root initiation by combining specific transcriptome data sets. *Plant Physiol*. 2010;153(1):34–40.
48. Bardou F, Ariel F, Simpson CG, et al. Long noncoding RNA modulates alternative splicing regulators in Arabidopsis. *Dev Cell*. 2014;30(2):166–176.
49. Trincado JL, Entizne JC, Hysenaj G, et al. SUPPA2: Fast, accurate, and uncertainty-aware differential splicing analysis across multiple conditions. *Genome Biol*. 2018;19(1):40.
50. Zhang R, Kuo R, Coulter M, et al. A high-resolution single-molecule sequencing-based Arabidopsis transcriptome using novel methods of iso-seq analysis. *Genome Biol*. 2022;23(1):149.
51. Bray NL, Pimentel H, Melsted P, Pachter L. Near-optimal probabilistic RNA-seq quantification. *Nat Biotechnol*. 2016;34(5):525–527.

SUPPORTING INFORMATION

Additional supporting information can be found online in the Supporting Information section at the end of this article.

How to cite this article: Roulé T, Legascue MF, Barrios A, Gaggion N, Crespi M, Ariel F, et al. The long intergenic noncoding RNA *ARES* modulates root architecture in Arabidopsis. *IUBMB Life*. 2023;75(10):880–92. <https://doi.org/10.1002/iub.2761>